European Journal of AI, Computing & Informatics

Vol. 2 No. 1 2026

Article **Open Access**

LPDM-YOLOv8: A Lightweight Low-Light Object Detection Method Based on Laplacian Pyramid

Yahao Guo [1] and Dongxiang Fu [1,]

[1] University of Shanghai for Science and Technology, Yangpu District, Shanghai 200093, China
* Correspondence: Dongxiang Fu, University of Shanghai for Science and Technology, Yangpu District, Shanghai 200093, China

Received: 24 January 2026
Revised: 04 March 2026
Accepted: 15 March 2026
Published: 19 March 2026

Abstract: To address the performance degradation of YOLOv8 under low-light conditions, this paper proposes a lightweight low-light object detection method based on a Laplacian pyramid. A Laplacian Pyramid Dimming Module (LPDM) is integrated into YOLOv8 to construct an end-to-end detection framework with illumination-adaptive enhancement and multi-scale feature fusion. The proposed module performs brightness-aware adjustment and hierarchical detail reconstruction, effectively improving feature representation in dark scenes with negligible computational overhead. Experiments on the ExDark dataset show that LPDM-YOLOv8n achieves an mAP of 0.524, corresponding to an 8.0% relative improvement over the baseline YOLOv8n, while maintaining real-time performance at 32 FPS. Notably, only 16 additional parameters are introduced without increasing FLOPs. The results demonstrate that the proposed method significantly enhances detection robustness under low-light conditions while preserving efficiency, making it suitable for real-time applications.

Keywords: YOLOv8; Laplacian pyramid; LPDM; brightness adaptation; multi-scale feature fusion; real-time object detection

1. Introduction

Object detection is a fundamental task in computer vision and has been widely applied in autonomous driving, video surveillance, and robotic navigation. Although deep learning-based detectors have achieved remarkable progress in accuracy and efficiency, their robustness remains limited under challenging conditions such as low-light environments. In low-light scenarios, images often suffer from noise amplification, reduced contrast, and detail loss, which significantly degrade detection performance [1]. Therefore, enhancing detection robustness under insufficient illumination has become an important research topic.

Modern real-time object detection frameworks, represented by the YOLO series [2], achieve a favorable balance between accuracy and computational efficiency. However, most detectors are trained under normal lighting conditions and exhibit noticeable performance degradation when directly applied to low-light scenes. To evaluate detection performance in dark environments, the ExDark dataset was proposed, providing a benchmark specifically designed for low-light object detection [3].

Existing low-light enhancement methods are mainly based on Retinex theory or learning-based approaches such as Zero-DCE [4,5]. While these methods improve visual quality, they are typically designed for image enhancement rather than detection tasks, and may introduce additional computational overhead when integrated into real-time

detection pipelines. To address low-light detection directly, methods such as PE-YOLO incorporate enhancement modules into detection networks [6]. Although performance gains are achieved, increased structural complexity often affects inference speed. Furthermore, multi-scale feature representation techniques, such as Feature Pyramid Networks (FPN), have demonstrated the importance of hierarchical feature fusion for improving detection robustness, yet illumination-adaptive multi-scale enhancement remains insufficiently explored [7].

2. Introduction to the LPDM Module

The LPDM module consists of three components: the brightness calculation module (CB), the Pyramid Mosaic Image Enhancer (PMIE), and the Laplacian Pyramid Decomposition module (PD), as illustrated in Figure 1.

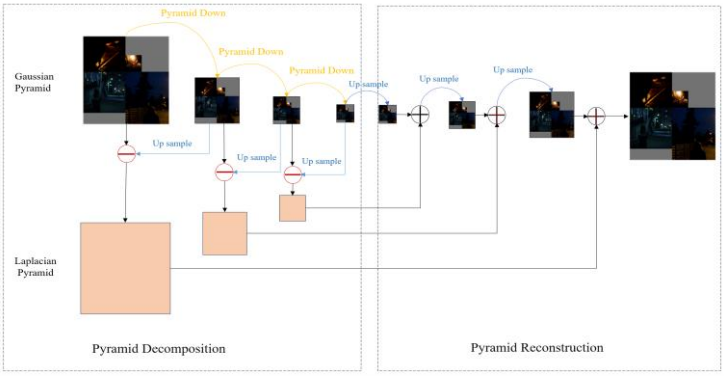

Figure 1. LPDM overall structure diagram.

First, the CB module computes the average brightness of the input image. If the brightness is within the normal range, the image is directly forwarded through Path 1 to the subsequent detection network. Otherwise, the image is identified as low-light and processed through Paths 2-4.

In Path 2, the original low-light image is directly forwarded to the final fusion stage to preserve intrinsic image information.

In Path 3, the low-light image is decomposed by the PD module into multi-scale representations to extract structural and detail features.

In Path 4, the image is first segmented by PMIE for region-wise enhancement. The CB module computes sub-image brightness parameters, and the IE module performs adaptive brightness and contrast adjustment. The enhanced image is then decomposed by the PD module.

The multi-scale features obtained from Paths 3 and 4 are fused layer by layer using a 1:1 weighting strategy and reconstructed into an enhanced RGB image. Finally, this reconstructed image is combined with the original low-light image from Path 2 to generate the final output, which is then fed into the YOLO detection network.

2.1. PMIE Module

PMIE is an image enhancement module specifically designed for Mosaic data-augmented images. Its core principle lies in decomposing the input image into n×n sub-images through a segmentation module. The brightness calculation module (CB) is then employed to evaluate the brightness parameters of each sub-image. Subsequently, the image enhancement module (IE) performs brightness and contrast optimization on each sub-image. Finally, the enhanced sub-images are recombined into a complete image through a reconstruction module and fed into the subsequent network for processing. This method effectively improves the model's performance in processing Mosaic images

under low-light conditions. By adopting a region-wise enhancement strategy, it prevents information loss in local regions caused by excessive processing.

The CB module is used to calculate the average brightness of images after Mosaic data augmentation. As illustrated in Figure 1, the input of LPDM is the image processed by Mosaic data augmentation within the YOLO framework. Mosaic data augmentation generates diversified training samples through multi-scale image stitching. Specifically, four images are randomly selected from the dataset and placed onto a blank canvas of fixed size in a 2 × 2 layout, where the four images are positioned in the four quadrants of the canvas to form a new composite image. Since the sizes of the selected images may vary, the uncovered regions of the canvas are filled with a fixed gray value of 144, which corresponds to the mid-level brightness in the value channel of the HSV color space. The calculation principle of the CB module is as follows: first, the brightness of each pixel is computed according to the following formula:

$$I_{pixel} = 0.299 * R + 0.587 * G + 0.114 * B \tag{1}$$

Where I_{pixel} represents the brightness value of a single pixel, and R, G, and B denote the red, green, and blue channel values, respectively. This formula is based on the ITU-R BT.601 standard, where the coefficients (0.299, 0.587, 0.114) simulate the characteristics of human visual perception. Subsequently, all pixel brightness values are normalized to the range of 0 to 255. According to Formula (2), the average brightness of the entire image is calculated to obtain the effective mean brightness of the image.

$$I_{image} = \frac{1}{H \times W} \sum_{i}^{H} \sum_{j}^{W} I_{pixel}(i, j) \tag{2}$$

Where I_{image} represents the average brightness value of the entire image.(H, W)denote the height and width of the image (in pixels),and Ipixel(i, j) represents the brightness value of the pixel located at the i-th row and j-th column.

The IE module in PMIE is responsible for adjusting image brightness, contrast, and sharpness. The basic principle of brightness adjustment is based on the weighted combination of input image pixel values.

The enhancement process in IE includes brightness adjustment and contrast adjustment performed separately. The brightness adjustment is calculated according to Formula (3):

$$I_1 = \alpha \cdot I_0 \tag{3}$$

The contrast adjustment is given by Formula (4):

$$I_2 = \beta \cdot I_1 + (1 - \beta) \cdot Avg(I_1) \tag{4}$$

Here, I_0 denotes the input image, α is the brightness adjustment factor, and β is the contrast adjustment factor. These two parameters are adaptively adjusted based on the average brightness of the image. I_1 represents the image after brightness enhancement and serves as the input for the contrast calculation formula. Avg(I_1) denotes the mean grayscale value of I_1,and I_2 is the final enhanced image.

2.2. PD Module.

The function of the PD module is to extract low-frequency and high-frequency information from the original image and the image enhanced by PMIE through Laplacian pyramid decomposition. Specifically, it first constructs a Laplacian pyramid and analyzes each layer to extract image features at different scales. Among them, low-frequency information mainly reflects the overall structure and general contours of the image, while

high-frequency information contains detailed and edge features, as shown in Figure 2.

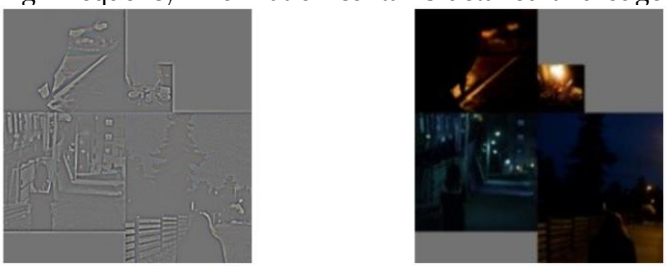

Figure 2. High-frequency and low-frequency components of an image. (a) High-frequency information. (b) Low-frequency information.

The Laplacian image pyramid is constructed by creating a series of images with different levels of detail. First, a Gaussian pyramid is generated for each input image. The Gaussian pyramid is constructed by repeatedly applying low-pass filtering and downsampling operations to the image. Each layer of the Gaussian pyramid represents low-frequency information at a specific scale. By computing the difference between each layer of the Gaussian pyramid and its upsampled version, the Laplacian image pyramid can be obtained. The Laplacian pyramid decomposition can be expressed as follows:

$$L_i = G_i - Upsample\left(G_{i+1}\right) \tag{5}$$

Where L_i denotes the image at the i-th layer of the Laplacian pyramid,G_i represents the image at the i-th layer of the Gaussian pyramid,and Upsample() denotes the upsampling operation. The reconstruction process of the Laplacian pyramid can be expressed as follows

$$G_i = L_i + Upsample\left(G_{i+1}\right) \tag{6}$$

The pyramid decomposition and reconstruction processes are illustrated in Figure 3.

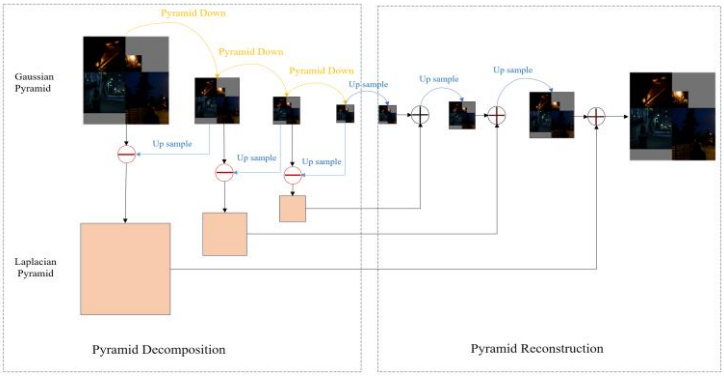

Figure 3. Laplace pyramid decomposition and reorganization.

2.3. Fusion

The fusion process of LPDM involves combining the corresponding layers of the Laplacian pyramids of the original image and the enhanced image using a 1:1 weighted ratio, followed by image reconstruction using the Gaussian pyramid of the original image. This process ensures that the information of the original image is preserved while effectively extracting feature information from low-light images. Such a fusion strategy not only enhances the representation of image details but also improves visibility under low-light conditions, thereby providing effective data for subsequent object detection tasks. The detailed structure of the fusion module is shown in Figure 4.

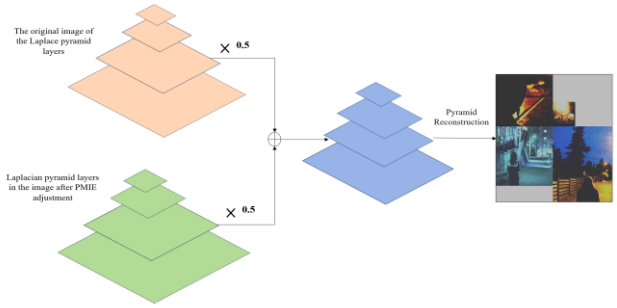

Figure 4. Details of Fusion module.

3. Experiments

3.1. Datasets and Experimental Setup.

The ExDark dataset is employed for training and evaluation, with an 8:1:1 split for training, validation, and testing. Multi-scale training and data augmentation techniques, including Mosaic and MixUp, are applied to enhance model robustness. All images are resized to 640 × 640 pixels before being fed into the network. The model is implemented using PyTorch 1.13.1 and trained on an RTX 4060 GPU. The SGD optimizer is adopted with a learning rate of 0.01, momentum of 0.8, weight decay of 0.0005, and a batch size of 8, for a total of 150 training epochs. During evaluation, test-time augmentation is utilized, and mAP is calculated with IoU thresholds ranging from 0.5 to 0.95.

3.2. Experiments on Public Datasets.

The per-class mAP@0.5:0.95 and overall performance comparisons are summarized in Table 1. Compared with YOLOv8n and other representative low-light enhancement modules, LPDM-YOLOv8n achieves the highest overall mAP of 0.524 and demonstrates consistent improvements across most object categories. In addition, it maintains the fastest inference speed (32 FPS), indicating a superior balance between detection accuracy and real-time efficiency under low-light conditions (Table 2).

Table 1. Comparison of Low-Light Enhancement Modules within YOLOv8n on ExDark.

Model	Bicycle	Boat	Bottle	Bus	Car	Cat	Chair	Cup	Dog	Motorbike	People	Table	MAP	FPS
YOLOv8n	0.579	0.416	0.529	0.673	0.543	0.449	0.387	0.519	0.507	0.468	0.422	0.322	0.485	32
PENet-YOLOV8n	0.533	0.433	0.522	0.689	0.530	0.477	0.369	0.513	0.477	0.465	0.428	0.341	0.491	28
SCInet-YOLOV8n	0.542	0.427	0.535	0.693	0.539	0.473	0.384	0.529	0.482	0.438	0.421	0.338	0.489	28
IAT-YOLOV8n	0.536	0.423	0.529	0.685	0.536	0.486	0.375	0.512	0.476	0.461	0.431	0.336	0.492	26
LPDM-YOLOV8n	0.547	0.428	0.555	0.699	0.547	0.483	0.39	0.527	0.491	0.474	0.437	0.343	0.524	32

Table 2. Performance comparison of different YOLO models on the ExDark dataset.

model	mAP@0.5:0.95	FPS	Parameters	GLOPS
YOLOV5s	0.448	26	7083577	16.4
YOLOv8n	0.485	32	2686772	6.8
YOLOV10n	0.485	29	2699096	8.2
YOLOV11n	0.398	31	2584492	6.8

LPDM -YOLOv8n	0.524	32	2686788	6.8

The comprehensive comparison results are summarized in Table 2. LPDM-YOLOv8n achieves the highest mAP@0.5:0.95 of 0.524 among all evaluated models while maintaining real-time inference at 32 FPS. Compared with the baseline YOLOv8n, the proposed LPDM introduces only 16 additional parameters without increasing computational complexity (6.8 GFLOPs). These results indicate that the proposed method effectively improves detection accuracy under low-light conditions while preserving efficiency.

To analyze the impact of the LPDM module on feature attention under low-light conditions, eight images from the ExDark dataset are randomly selected for heatmap visualization. The activation maps generated by YOLOv8n and LPDM-YOLOv8n are shown in Figure 5. As illustrated in Figure 5, LPDM-YOLOv8n exhibits stronger and more concentrated responses on target regions, with reduced background interference compared to YOLOv8n.

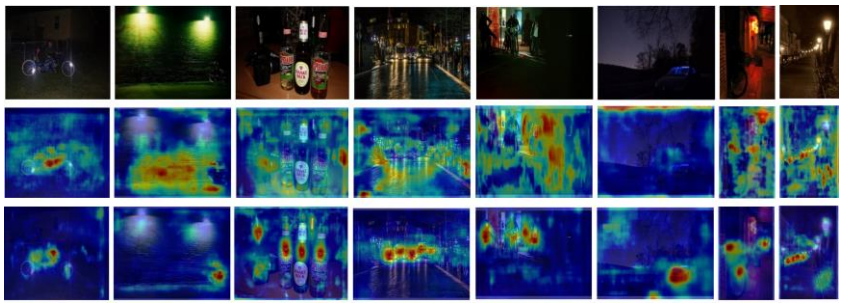

Figure 5. Heatmap visualization of detection results for the original image, YOLOv8n, and LPDM-YOLOv8n. (a) Original image. (b) YOLOv8n detection heatmap. (c) LPDM-YOLOv8n detection heatmap.

Figure 6 further presents qualitative detection comparisons between YOLOv8n and LPDM-YOLOv8n on several representative images, demonstrating improved localization accuracy and detection confidence under low-light conditions.

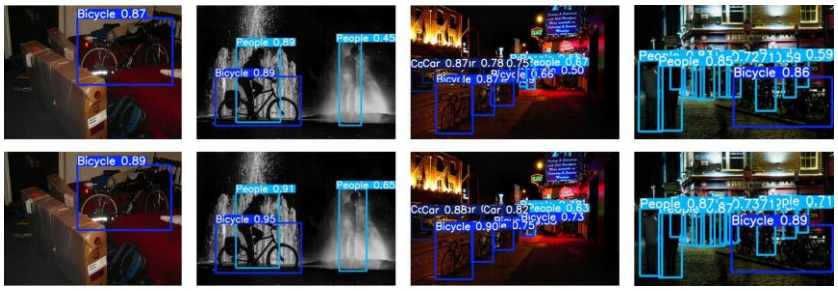

Figure 6. Qualitative comparison of detection results produced by YOLOv8n and LPDM-YOLOv8n on randomly selected images. (a) YOLOv8n results. (b) LPDM-YOLOv8n results.

Figure 7 illustrates the qualitative enhancement results of different methods, highlighting the visual differences between the proposed LPDM and existing approaches.

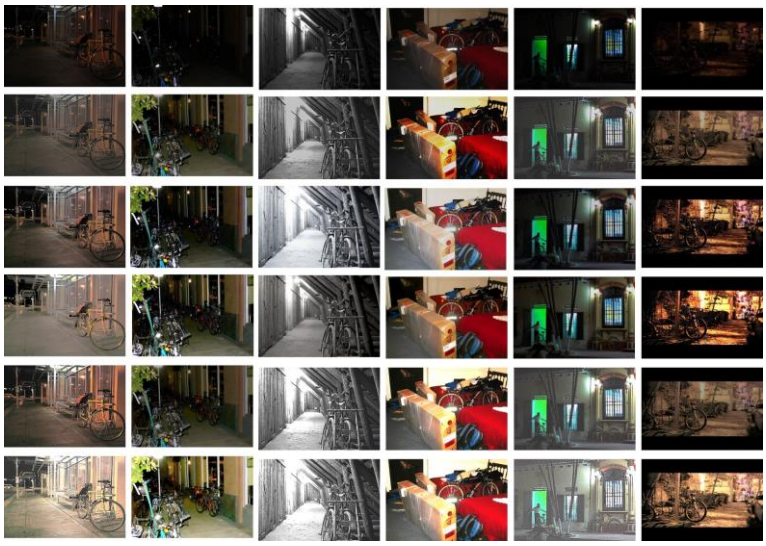

Figure 7. Visual comparison of images enhanced by different methods. (a) Original image. (b) SCINet. (c) Zero-DCE. (d) RetinexNet. (e) MBLLEN. (f) LPDM.

3.3. Comparative Experiments with Other Illumination Adjustment Modules

In this section, the proposed LPDM is compared with representative low-light enhancement methods, including SCINet, ZeroDCE, RetinexNet, and MBLLEN, using PSNR, SSIM, and NIQE as evaluation metrics. These metrics measure image quality in terms of distortion, structural similarity, and visual naturalness, respectively. As shown in Table 3, LPDM achieves the best overall performance across all major metrics. Specifically, LPDM obtains the highest PSNR of 25.795 dB and SSIM of 0.766, indicating superior distortion reduction and structural preservation. Meanwhile, LPDM achieves the lowest NIQE value of 2.905, demonstrating improved visual quality and noise suppression. In addition to quality improvement, LPDM exhibits remarkable computational efficiency. The average processing time is only 4.021 ms per image, which is significantly lower than that of RetinexNet and MBLLEN, and even faster than ZeroDCE. These results confirm that LPDM effectively balances enhancement performance and real-time efficiency, making it suitable for practical low-light detection applications.

Table 3. Image quality evaluation on the Exdark dataset.

	PSNR（dB）	SSIM	NIQE	Time（ms）
Original image	—	1.000	3.351	—
SCINet	9.113	0.377	3.980	10.681
ZERODCE	12.82	0.475	3.705	5.740
RetinexNet	10.991	0.433	4.999	169.032
Mbllen	15.701	0.587	3.056	221.453
LPDM	25.795	0.766	2.905	4.021

3.4. Ablation Experiments

To verify the effectiveness of each component in LPDM, ablation experiments are conducted in this study, and the results are presented in Table 4. In the table, "√" indicates that the corresponding module is enabled. When only the IE module is used to enhance the entire Mosaic image, the model achieves an mAP@0.5:0.95 of 0.431, indicating limited performance improvement. After introducing sub-image segmentation and recombination to form PMIE, the mAP increases to 0.487, demonstrating that region-wise processing helps reduce global brightness estimation errors. With the further

incorporation of the CB module for brightness-adaptive selection, the mAP is improved to 0.524, indicating that CB effectively prevents excessive enhancement of normally illuminated images. Throughout the ablation process, the model's FPS remains nearly unchanged, confirming that LPDM satisfies real-time requirements while enhancing detection performance.

Table 4. Contributions of each component in LPDM.

IE	PMIE	CB	mAP@.5	FPS
√	—	—	0.431	35
√	√	—	0.487	32
√	√	√	0.524	32

4. Conclusion

With the growing demand for object detection in unmanned systems, intelligent surveillance, and industrial vision, achieving high accuracy and real-time performance under low-light conditions has become increasingly important. To address the issues of insufficient brightness, detail degradation, and performance decline in low-light environments, this paper proposes a lightweight Laplacian pyramid-based enhancement module integrated into YOLOv8 in an end-to-end framework.

Experimental results on the ExDark dataset demonstrate that LPDM-YOLOv8 achieves an mAP@0.5:0.95 of 0.524, corresponding to an 8.0% relative improvement over the baseline while maintaining real-time inference at 32 FPS with negligible computational overhead. These results confirm that the proposed method effectively enhances detection robustness in low-light scenarios without sacrificing efficiency.

Future work will extend validation to larger-scale low-light datasets and further optimize the model structure according to diverse illumination characteristics to improve adaptability in complex environments.

References

1. C. Chen, Q. Chen, J. Xu, and V. Koltun, "Learning to see in the dark," In *Proceedings of the IEEE conference on computer vision and pattern recognition*, 2018, pp. 3291-3300. doi: 10.1109/cvpr.2018.00347
2. J. Redmon, S. Divvala, R. Girshick, and A. Farhadi, "You only look once: Unified, real-time object detection," In *Proceedings of the IEEE conference on computer vision and pattern recognition*, 2016, pp. 779-788. doi: 10.1109/cvpr.2016.91
3. Y. P. Loh, and C. S. Chan, "Getting to know low-light images with the exclusively dark dataset," *Computer vision and image understanding*, vol. 178, pp. 30-42, 2019. doi: 10.1016/j.cviu.2018.10.010
4. D. J. Jobson, Z. U. Rahman, and G. A. Woodell, "A multiscale retinex for bridging the gap between color images and the human observation of scenes," *IEEE Transactions on Image processing*, vol. 6, no. 7, pp. 965-976, 1997.
5. C. Guo, C. Li, J. Guo, C. C. Loy, J. Hou, S. Kwong, and R. Cong, "Zero-reference deep curve estimation for low-light image enhancement," In *Proceedings of the IEEE/CVF conference on computer vision and pattern recognition*, 2020, pp. 1780-1789.
6. X. Yin, Z. Yu, Z. Fei, W. Lv, and X. Gao, "Pe-yolo: Pyramid enhancement network for dark object detection," In *International conference on artificial neural networks*, September, 2023, pp. 163-174. doi: 10.1007/978-3-031-44195-0_14
7. T. Y. Lin, P. Dollár, R. Girshick, K. He, B. Hariharan, and S. Belongie, "Feature pyramid networks for object detection," In *Proceedings of the IEEE conference on computer vision and pattern recognition*, 2017, pp. 2117-2125.